

Praziquantel systems with improved dissolution rate obtained by high pressure homogenization

M.A. Gonzalez^{a,b}, M.V. Ramírez Rigo^{a,b}, N.L. Gonzalez Vidal^{a,c,*}

^a Departamento de Biología, Bioquímica y Farmacia, Universidad Nacional del Sur (UNS), San Juan 670, 8000 Bahía Blanca, Argentina

^b Planta Piloto de Ingeniería Química (PLAPIQUI), UNS-CONICET, Camino La Carrindanga Km 7, 8000 Bahía Blanca, Argentina

^c Consejo Nacional de Investigaciones Científicas y Técnicas (CONICET), Camino La Carrindanga Km 7, 8000 Bahía Blanca, Argentina



ARTICLE INFO

Keywords:

Praziquantel

High pressure homogenization

Dissolution rate

ABSTRACT

Praziquantel (PZQ), an anthelmintic agent commonly administered to humans and cattle, has low aqueous solubility, which compromises its bioavailability and efficacy. The purpose of this study was to develop a new formulation, in order to improve PZQ dissolution rate. PZQ dispersions have been developed by high-pressure homogenization (HPH) using different stabilizers, selected upon PZQ saturation solubility. After the screening, two promising formulations were developed, combining poloxamer 188 with polyvinylpyrrolidone or maltodextrin. Characterization studies including particle size distribution, crystallinity, morphology, drug content, and in vitro dissolution profiles, were performed over selected formulations. The scanning electronic micrographs revealed that the morphology of suspended particles corresponded to elongated shapes, with an average particle size close to the micron range. X-ray powder diffractometry and differential scanning calorimetry results confirmed the drug crystallinity, before and after the HPH process. Besides, differential scanning calorimetry revealed the absence of interactions between PZQ and excipients. The dissolution rate of PZQ dispersions was significantly enhanced compared with raw PZQ, either in phosphate buffer or hydrochloric acid, mainly due to particle size reduction, thus improved saturation solubility.

1. Introduction

The anthelmintic Praziquantel (PZQ) is a broad-spectrum agent classified as a pyrazinoisoquinoline [1]. PZQ presents a considerably high activity against trematodes and tapeworms, including all *Schistosoma* species and *Taenia solium*, which is the agent responsible for cysticercosis disease in its larval phase [2]. Although it is considered an effective, safe, and low-cost drug, its usefulness is limited due to its low water solubility (only 0.04 g/100 mL) and its important first pass effect [3–5]. Nevertheless, this agent is widely used in developing countries for the treatment of various parasitic diseases that cause morbidity, both in man and in cattle [6]. An improvement of those unfavorable properties would promote a more effective and rational pharmacotherapeutic scheme.

PZQ is classified in the Biopharmaceutical Classification System (BCS) as a class II active pharmaceutical ingredient, which implies that the drug presents low aqueous solubility and high permeability through the intestinal membrane [7]. Moreover, due to its low solubility and high metabolism, in the Biopharmaceutics Drug Disposition Classification System (BDDCS), it is also classified as a type II drug [8]. It is well

known that only the dissolved fraction of the drug will be available to be absorbed, and exert a therapeutic effect. Due to those unfavorable properties, these drugs may present significant oral absorption problems, which could lead to a compromised bioavailability [9]. A possible approach for overcoming the low water solubility issue is to reduce the drug particle size, especially below the micrometer range, leading to the enhancement of the specific surface area, the saturation solubility and, thus, the dissolution rate [10]. The Noyes-Whitney equation clearly states the dependence between these variables [11]. Moreover, the influence of PZQ systems with reduced particle size on the cysticerci metabolism was previously established [12].

A well-established procedure to reduce particle size is high-pressure homogenization (HPH), a top-down methodology, which is widely applied in food, cosmetic, and pharmaceutical industries [13]. The advantages of this technology include ease of operation and industrial scaling up, ability to be applied to several active pharmaceutical ingredients, avoidance of harsh solvents, and reduction of product contamination [14]. Moreover, compared with other size reduction techniques, HPH has no drug loading evaluation concern, since all active pharmaceutical ingredients added will be present in the final

* Corresponding author at: Departamento de Biología, Bioquímica y Farmacia, Universidad Nacional del Sur (UNS), San Juan 670, 8000 Bahía Blanca, Argentina.
E-mail addresses: alejandra.gonzalez@uns.edu.ar (M.A. Gonzalez), vrrigo@plapiqui.edu.ar (M.V. Ramírez Rigo), nlgvidal@uns.edu.ar (N.L. Gonzalez Vidal).

<https://doi.org/10.1016/j.msec.2018.07.050>

Received 14 September 2017; Received in revised form 4 June 2018; Accepted 19 July 2018

Available online 20 July 2018

0928-4931/ © 2018 Elsevier B.V. All rights reserved.

formulation. Nevertheless, the reduced size of the nanoparticles and the associated high surface energy entails a high probability of obtaining systems with physical instability, which is the major drawback of this technique [15].

The suspension, consisting of a drug, a stabilizing agent, and a liquid dispersion medium, is forced through a very small gap under pressure, with a significantly high velocity. During the process, particle size reduction is achieved because of shear and cavitation forces, and inter-particle collisions. Smaller particle size and narrower distributions can be obtained by the increase of pressure and/or number of cycles in the HPH process [10]. Critical points of this technique include the suitable selection of stabilizer type, and concentration of both drug and stabilizer, in order to achieve an adequate size reduction and improve the physical stability of obtained formulations [16,17]. The most common approaches to impart repulsive forces or energy barriers are steric and/or electrostatic techniques. Steric stabilization can be obtained by adsorption of polymers (e.g., cellulose derivatives, polyvinylpyrrolidone, polyvinyl alcohol) or non-ionic surfactants (e.g., poloxamers, polysorbates) to the surface of the particle. On the other hand, electrostatic stabilization is achieved by adsorbing ionic surfactants (e.g., SLS) onto the particle surface [16,18]. However, in the case that dispersions of nanoparticles are intended to be post-processed as a dry powder, long-term stability of the liquid formulation is not a major concern. Finally, the characterization of the obtained system is crucial in the effective development of these formulations [10].

Multiple strategies have been carried out attempting to improve the solubility and dissolution rate of PZQ, e.g. solid dispersions, inclusion complexes with α -, β - and γ -cyclodextrins, solid lipid nanoparticles and polymeric nanoparticles, Poly (ϵ -caprolactone) implants, co-crystals by grinding methodology, microparticles, granules or coprecipitates [19–28]. Although these systems exhibited several advantages, important drawbacks could also be detected in the applied techniques, such as a greater process complexity, the use of organic solvents, a higher excipient proportion, and a drug loading estimation requirement or some matrix effects. However, to the best of our knowledge, the development of a suitable system for PZQ by HPH has not been studied.

The purpose of this study was to formulate novel dispersions of PZQ and selected stabilizers using the HPH technique, in order to improve the solubility and dissolution rate of the drug. The obtained formulations were subsequently characterized, regarding technological and crystallographic properties, such as particle size distribution, drug content, in vitro dissolution profiles, particle morphology, differential scanning calorimetry, and X-ray powder diffraction. Finally, all these properties were compared with the raw materials and their physical mixtures.

These novel systems, developed with a not complex and scalable technique, would promote the adoption of this technology in order to improve the properties of PZQ and parasitic diseases treatment.

2. Materials and methods

2.1. Materials

Pharmaceutical-grade PZQ was purchased from Todo Droga (Argentina), and complied with the British Pharmacopoeia requirements [29]. Selected stabilizers, including poloxamer 188 (P188 – Lutrol F68®), polyvinylpyrrolidone K30 (PVP – BASF), sodium lauryl sulfate (SLS – Lab. Cicarelli), and maltodextrin (MDX-Todo Droga), were pharmaceutical-grade quality. Dissolution media were prepared using analytical-grade potassium dihydrogen phosphate (Anedra-Research AG, Argentina), sodium hydroxide (Cicarelli, Argentina), and hydrochloric acid (HCl - Anedra Research AG, Argentina). Different types of water were used: triple distilled for the formulation of PZQ dispersions, deionized for dissolution media preparation, and Ultra-purified Milli-Q® (Millipore SAS, France) for dilution of samples during particle size analysis. For PZQ assay, ethanol analytical grade (Dorwil,

Argentina) was used.

2.2. Methods

2.2.1. Physical mixtures preparation

For physical mixtures (PM) preparation, PZQ and stabilizers were thoroughly mixed in a glass mortar, considering the same drug/stabilizer ratios (w/w) as for the PZQ dispersions.

2.2.2. Saturation solubility studies

The HPH process is sensitive to the proper selection of stabilizers and drug concentration [16]. Excipients were selected based on their stabilization properties (i.e., steric [PVP, MDX], electrostatic [SLS] or a combination of polymeric/surface active agents [P188]). These four water-soluble compounds are approved as inactive ingredients by the U.S. Food and Drug Administration (FDA), and commonly used for the formulation of drug delivery systems [30]. In general, they exhibit good binding ability on the surface of drug particles, and affinity to hydrophobic and hydrophilic areas [31]. In particular, it has been reported that interactions between PZQ and PVP are mostly van der Waals forces [32].

Moreover, the solubility of the formulated drug in the stabilizer solution plays an important role in the particle size increase during storage, in terms of Ostwald ripening [33]. Therefore, the stabilizer should have a slight effect on drug solubility [33]. For that reason, it is critical to determine the solubility of the drug in different stabilizer solutions, in order to establish the PZQ supersaturation concentration required. Binary stabilizer solutions were prepared at a total concentration of 1% (w/v). These binary solutions consisted of a combination of P188 with SLS, PVP or MDX, in a 1:1 ratio. Moreover, P188 was used individually (1% w/v). An excess of PZQ was added to 7 mL of stabilizer solutions ($n = 3$), and the mixtures were stirred for 96 h at 40 °C (the highest temperature reached by the dispersion during the HPH process). The concentration of PZQ was determined at 264 nm (Varian Cary 50Conc, Varian Instruments, Australia), after centrifugation (3500 rpm, 15 min) and filtration (0.45- μ m pore-size nylon membrane, Microclar, Argentina) of the samples. At the PZQ maximum absorption wavelength, no interference signals were recorded for stabilizer solutions. Statistical evaluation of solubility results was performed using Analysis of Variance (ANOVA) followed by LSD multiple comparisons. Significance was tested at the 0.05 level of probability (p).

2.2.3. Preparation of PZQ dispersions

PZQ (2 g), as supplied, was dispersed within the stabilizer solution at a concentration of 1% (w/v), in a final volume of 200 mL. The drug:stabilizer ratio was 1:1 (w/w), i.e. the concentration of stabilizer was 1% (w/v) in the case of F1, and 0.5% per each stabilizer in the case of F2-F4 (Table 1). The suspensions were stirred at 1000 rpm for 10 min. To avoid obstruction of the homogenization valve, a first size-reduction step was needed [10]. Therefore, mixtures were pre-homogenized at 22,000 rpm for 10 min (PRO Scientific PRO250). The obtained suspensions were then processed by HPH (APV 1000, Denmark) for 60 cycles at 950 bar.

Table 1
Formulated PZQ systems.

Sample	Stabilizer mixture ^a
F1	P188
F2	P188-SLS
F3	P188-MDX
F4	P188-PVP

^a API concentration of 1% (w/v) and a PZQ:stabilizer mixture ratio of 1:1.

2.2.4. Particle size distribution analysis

Particle size distribution analysis of PZQ dispersions was performed by photon correlation spectroscopy (PCS). This technique yields accurate results in the range of 2 nm to 3 μm [10,34]. On the other hand, laser diffraction (LD) was employed to evaluate particle size distribution of non-treated PZQ, with a measuring range up to 2000 μm [10].

The particle size distribution of PZQ dispersions was determined using a Zetasizer Nano ZS90 (Malvern Instruments, UK). Samples were backscattered by a helium-neon laser (633 nm), at an angle of 90°, and a constant temperature of 25 °C. Each sample was analysed immediately after its formulation ($n = 3$). Before measurements, a drop of PZQ dispersion was suitably diluted using ultrapurified water, in order to achieve the required particle density for PCS analysis and results independent of particle concentration. The diameters reported were calculated using volume weighted distribution. The median particle size by volume D_{50} (i.e., the maximum particle diameter below which half of the sample volume exists), D_{90} , and D_{95} were used as characterization parameters.

For comparison purposes, particle size analysis of raw material was conducted by LD (HORIBA LA950-V2, Japan), using the unit equipped with a powder jet dry feeder system at 0.2 MPa airflow. The volume weighted particle size distributions were obtained ($n = 3$), using D_{10} , D_{50} , and D_{90} as characterization parameters, associated with its corresponding standard deviation (SD).

2.2.5. Crystalline state evaluation

To evaluate possible internal structure modifications during the application of HPH, crystalline state evaluation was conducted, before and after particle size reduction process, by differential scanning calorimetry (DSC) and powder X-ray diffraction (XRPD) analysis. In order to obtain a powder, PZQ dispersions were dried at 40 °C in a thermostatically controlled oven.

DSC analysis was performed on raw PZQ, stabilizers, PMs, and dried dispersions, using a differential scanning calorimeter (Perkin Elmer Pyris1, USA). Approximately 8 mg of each sample was scanned from 20 to 200 °C, at a heating rate of 10 °C/min, in aluminum-crippled pans under nitrogen gas flow. An empty aluminum pan was used as the standard reference.

Moreover, the physical state of stabilizers and PZQ in the different samples (raw material, PMs, and dispersions) was evaluated using a diffractometer (D/Max IIIc, Japan), with a Ni-filtered $\text{CuK}\alpha$ radiation detector ($k\lambda$ 1.5405 Å). It was operated at a voltage of 35 kV and a current of 15 mA, in the 2θ range from 2.5° to 60°, with a scan angular speed of 2° min^{-1} and a scan step of 0.02°.

2.2.6. Scanning electronic microscopy

The surface morphologies of raw materials (PZQ and stabilizers), PMs, and dispersions were investigated by scanning electron microscopy (SEM - LEO EVO 40-XVP, Germany). Raw material and PMs were evaluated as supplied or prepared, respectively. In the case of PZQ dispersions, a drop was dispersed onto glass coverslips, and the water was left to evaporate naturally. The obtained powder was fixed on aluminum stubs using double-sided adhesive tape and coated with Au in a sputter coater (PELCO 91000, USA). All raw material (PZQ and stabilizers) and PMs micrographs were recorded at 300 \times , and dispersions micrographs were recorded at 20,000 \times .

2.2.7. In vitro dissolution studies

In vitro dissolution studies on raw PZQ (100 mg) and formulated dispersions F3 and F4 (10 mL) were performed using the paddle method (Erweka DT60, Germany) at 50 rpm and 37.0 \pm 0.5 °C ($n = 3$). At 5, 15, 30, and 60 min, 10 mL samples were withdrawn (replacing an equal volume of fresh medium) and filtered using a 0.45 μm pore-size nylon membrane (Gamafil, Argentina). The amount of PZQ dissolved was determined by UV spectrophotometry at 264 nm, and referred to real drug content in each sample (also assessed by UV analysis, in ethanol,

using a calibration curve constructed for this purpose). For dissolution profiles construction, the mean percentage of PZQ dissolved and SD were reported.

The dissolution medium described for PZQ tablets analysis consists of 0.1 N HCl containing 2.0 mg of SLS per mL [35]. With this great amount of surfactant, it is difficult to observe differences between the dissolution profiles of raw material and formulated dispersions. Therefore, in vitro dissolution profiles were carried out in 900 mL of 0.1 N HCl without SLS, in order to obtain better discriminant conditions. Besides, to evaluate the dissolution behaviour in a physiologically relevant pH, the test was also performed in pH 7.4 phosphate buffer solution (PB), prepared according to USP requirements [35]. According to previous studies performed in our laboratory, carried out applying similar methodology of Section 2.2.2, PZQ solubility in dissolution media at 37 °C is 0.524 \pm 0.013 for PB and 0.677 \pm 0.067 for 0.1 N HCl. Considering this solubility data, and the amount of sample used for dissolution testing, sink conditions were assured.

Dissolution profiles were compared using ANOVA, in terms of dissolution rate constant (k) and Dissolution Efficiency (D.E.). D.E. is defined as the area under the dissolution curve up to a certain time t , expressed as a percentage of the area of the rectangle described by 100% dissolution, at the same time [36]. A p -value $<$ 0.05 was considered to be significant.

3. Results and discussion

3.1. Saturation solubility studies

PZQ solubility, in triple distilled water at 40 °C, was 0.332 \pm 0.018 mg/mL. The PZQ solubility results in stabilizer solutions without SLS were 0.336 \pm 0.019 (PZQ dispersed in P188), 0.367 \pm 0.063 (PZQ dispersed in P188-MDX), and 0.421 \pm 0.012 mg/mL (PZQ dispersed in P188-PVP). These samples showed no significant differences compared to the solubility of PZQ in water. In contrast, PZQ dispersed in a binary mixture of P188-SLS (1% w/v) exhibited a solubility value of 1.737 \pm 0.052 mg/mL, significantly higher than the value in water ($p <$ 0.01). It is worth emphasizing that conventional small-molecular weight surfactants (e.g., SLS) may excessively promote the dissolution of hydrophobic drugs, resulting in the destruction of crystalline structures (33). Therefore, to ensure supersaturation, the selection of stabilizer mixtures without SLS is a conservative condition for dispersions development.

3.2. Development and particle size distribution analysis of PZQ dispersions

The screening formulation compositions (F1–F4) are shown in Table 1.

Particle size distribution results, for PZQ dispersions and the raw material, are shown in Table 2. After 60 cycles of HPH, all formulations exhibited a particle size distribution below 2 μm , with highly significant

Table 2
Particle size distribution results^a.

Raw PZQ ^b	D_{10} (μm)	D_{50} (μm)	D_{90} (μm)
	8.24 \pm 0.3	18.63 \pm 0.8	102.31 \pm 29.9
Dispersions ^c	D_{50} (nm)	D_{90} (nm)	D_{95} (nm)
F1	1280.0 \pm 30.0	1726.7 \pm 32.1	1876.7 \pm 32.1
F2	1113.3 \pm 60.2	1456.7 \pm 73.7	1540.0 \pm 96.4
F3	891.0 \pm 66.2	1138.0 \pm 84.4	1214.0 \pm 102.1
F4	830.3 \pm 131.4	1063.3 \pm 193.5	1132.7 \pm 205.4

^a The values are shown as mean particle size \pm SD ($n = 3$).

^b LD measurements.

^c PCS measurements.

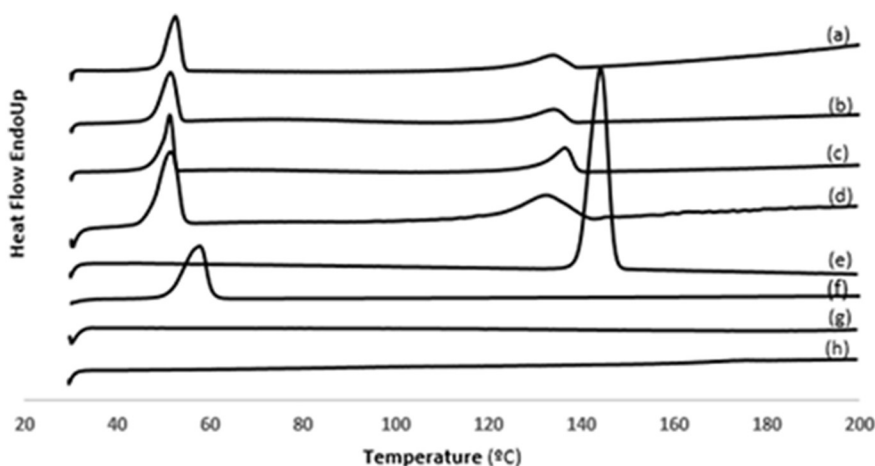


Fig. 1. DSC Thermograms

DSC thermograms for F3 dispersion(a), F4 dispersion (b), F3 PM (c), F4 PM(d), PZQ(e), P188 (f), MDX (g), and PVP (h).

reduction with respect to PZQ raw material (Table 2). However, the most effective particle size reduction was observed with the formulations containing MDX (F3) and PVP (F4), where half of the particle population (D_{50}) had a size below the micrometer range. Moreover, F2 exhibited a poor short-term physical stability, with rapid sedimentation of particles (visually inspected). For these reasons, only F3 and F4 were subsequently characterized.

3.3. Crystalline state evaluation

To evaluate possible crystalline structure modifications or appearance of amorphous patterns after HPH, DSC analysis were carried out on dried PZQ dispersions, and compared with raw materials and PMs (Fig. 1). PZQ exhibits only a single sharp endothermic peak, with an onset temperature of 139.4 °C and a maximum at 144.0 °C ($\Delta H = 100.9 \text{ J/g}$), corresponding to its melting point (Fig. 1e). These results are in agreement with the melting point and enthalpy of fusion described for the racemic form of the drug [27,28,37]. No other thermal events were recorded for the PZQ bulk drug.

As can be seen in Fig. 1f, P188 exhibited an endothermic peak at 57.6 °C, corresponding to its melting point, while PVP (Fig. 1h) showed a glass transition temperature at roughly 166.0 °C, in agreement with the results found in the literature [38,39]. Thermograms of MDX (Fig. 1g) did not show any significant event, such as glass transitions or melting endotherms, in the temperature range of 20 to 200 °C [40].

In the case of F3, the PM (Fig. 1c) exhibited two thermal events,

corresponding to the melting point of P188 and PZQ, at 51.2 °C and 136.4 °C respectively. For dried dispersions (Fig. 1a), the same peaks are observed at approximately the same temperatures (52.5 °C and 133.9 °C, respectively). For F4, both PM (Fig. 1d) and dispersions (Fig. 1b) also exhibited two thermal events, corresponding to P188 and PZQ melting peaks, at 51.3 °C and 132.0/133.8 °C respectively.

In both cases (F3 and F4), the particles exhibited a sharp endothermic melting peak, indicating the conservation of the crystalline structure of PZQ in the dispersions. It could be pointed out that the melting point of PZQ, in both PMs and dispersions, was slightly lower than the raw material. This might be due to a decrease in purity of individual components, or a partial dissolution of the drug in the melted excipient in the case of PM; and to the particle size reduction as predicted by the Gibbs–Thomson equation, in the case of PZQ dispersions [41–44]. On the other hand, even though the crystalline behaviour remained, a certain reduction in crystallinity percent was observed. Relative crystallinity of PZQ dispersions with respect to the raw material was calculated from the DSC data, by comparison of the area under the curve for the melting peak (ΔH), with results of 71.6% and 47.2% for F3 and F4 respectively. This behaviour agreed with observations made along other formulations and processing methods, where it is described that PVP has the ability to promote amorphous phase formation and inhibit crystal growth [9,19,45–50].

Crystallographic properties were also evaluated by XRPD (Fig. 2). As shown in Fig. 2e, sharp and intense diffraction peaks demonstrated the crystalline behaviour of raw PZQ. The XRPD pattern corresponded

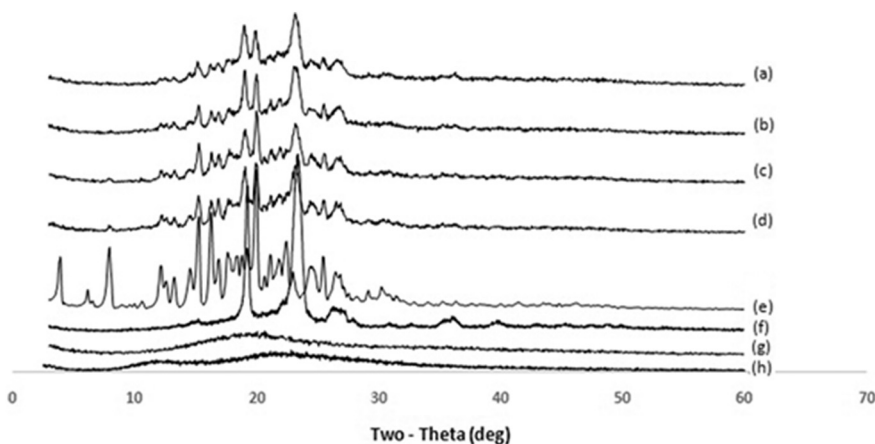


Fig. 2. X-ray diffractograms

X-ray diffractograms for F3 dispersion (a), F4 dispersion (b), F3 PM (c), F4 PM (d), PZQ (e), P188 (f), MDX (g), and PVP (h).

to that of PZQ racemate, both by the diffraction angles and by the intensity of the peaks, as reported by Liu et al. [37].

On the other hand, the excipients showed a crystalline state in the case of P188 (Fig. 2f), and an amorphous pattern in the case of PVP (Fig. 2h) and MDX (Fig. 2g), supporting the DSC results. The characteristic diffraction pattern of PZQ is conserved, both in PMs as dried dispersions of F3 and F4 (Fig. 2a–e). Although subtle differences in scattering intensity were observed, these results confirmed that the HPH technique retain the crystalline behaviour of PZQ (i.e., change from crystalline to amorphous), as it was also concluded for DSC analysis.

It is well known that the amorphous state exhibit greater instability and enhanced dissolution rates [51]. With time, high-energy amorphous particles could be transferred to low-energy crystalline form, depending on the temperature, type of stabilizer used, and the presence of the crystalline form [52]. Moreover, to prevent stability concerns, crystalline particles are preferable, considering the higher mobility of the drug in amorphous phases [53]. For these reasons, the developed formulations have a significant advantage.

3.4. Scanning electron microscopy

Shape and morphology of raw PZQ, excipients, PMs, and dispersions were evaluated using SEM analysis.

Raw PZQ drug presented a prismatic form with particles larger than 30 μm , which corresponded with the results obtained by LD (Fig. 3a). Both PVP (Fig. 3b), P188 (Fig. 3c), and MDX (Fig. 3d) exhibited a spherical shape. These results are in agreement with the literature [19,39,54].

In the case of PMs, F3 conformed an agglomerate containing large PZQ particles (Fig. 3g). The same occurs for F4, where the spherical particles of PVP and P188 can be distinguished, and the prismatic crystallites of PZQ were adsorbed on the surface of these polymers (Fig. 3e).

In the developed dispersions, particles maintained their prismatic shape, but the size was significantly decreased (Fig. 3f and h). Considering the broad particle size distribution visualized in the micrographs, similar particle sizes were observed in comparison with the PCS methodology. Nevertheless, more than 95% of the particle population was below 1214.0 nm and 1132.7 nm for F3 and F4, respectively (i.e., although a broad size distribution was obtained, the majority of PZQ particles measured around 1 μm). It should also be emphasized that after

the HPH process, particles retained the initial elongated shape, which might be advantageous for oral bioavailability, according to the results described by Banerjee et al. [55].

3.5. In vitro dissolution studies

Fig. 4a and b show the dissolution profiles of raw PZQ and dispersed formulations (F3–F4) in pH 7.4 PB and 0.1 N HCl, respectively. As it can be seen in both figures, the PZQ bulk drug did almost not dissolve after 60 min (5% dissolved in PB and 1% in HCl). In the case of PZQ dispersions, F4 showed a higher mean percentage dissolved result than F3, in both media, after 60 min of analysis (75% and 87% dissolved in PB and HCl, respectively, for F4, versus 57% and 66% dissolved for F3).

The obtained profiles were then adjusted to a first-order kinetics, and the constant rate k was calculated (Table 3). F4 showed the fastest dissolution rate (highest first order constant) and highest dissolution performance, in both media. Subsequently, a statistical comparison of profiles was performed, in terms of k and D.E. results (Table 3). Significant differences were recorded in all cases, both when comparing dissolution rate k and D.E. values of F3 and F4.

Modification of variables, such as a saturation solubility increase and a particle size reduction, lead to the improvement of drug dissolution rate, as is stated in Noyes–Whitney equation [11]. Therefore, the enhanced dissolution observed for PZQ dispersions could be attributed to the reduced particle size, associated with a higher surface area, and possible better contact between the active pharmaceutical ingredient and dissolution medium [56–58]. Additionally, the crystal habit might have a significant effect on in vitro dissolution behaviour. As described by Mengran Guo et al., rod nanocrystals reveal higher bioavailability and in vitro dissolution than spherical crystals, due to the larger surface area and small diffusion layer thickness exhibited by the former [59]. Moreover, amorphous solids have higher aqueous solubility than the corresponding crystalline state, due to differences in the lattice energies, leading to enhanced dissolution rates [60]. The improved dissolution performance observed for F4 relative to F3 could be ascribed to the lower crystallinity percent recorded for the former.

Finally, in comparison with other formulations described in the literature [19,26,27], the significant improvement in dissolution rate was achieved using a not complex (one-step), organic solvent-free and scalable methodology.

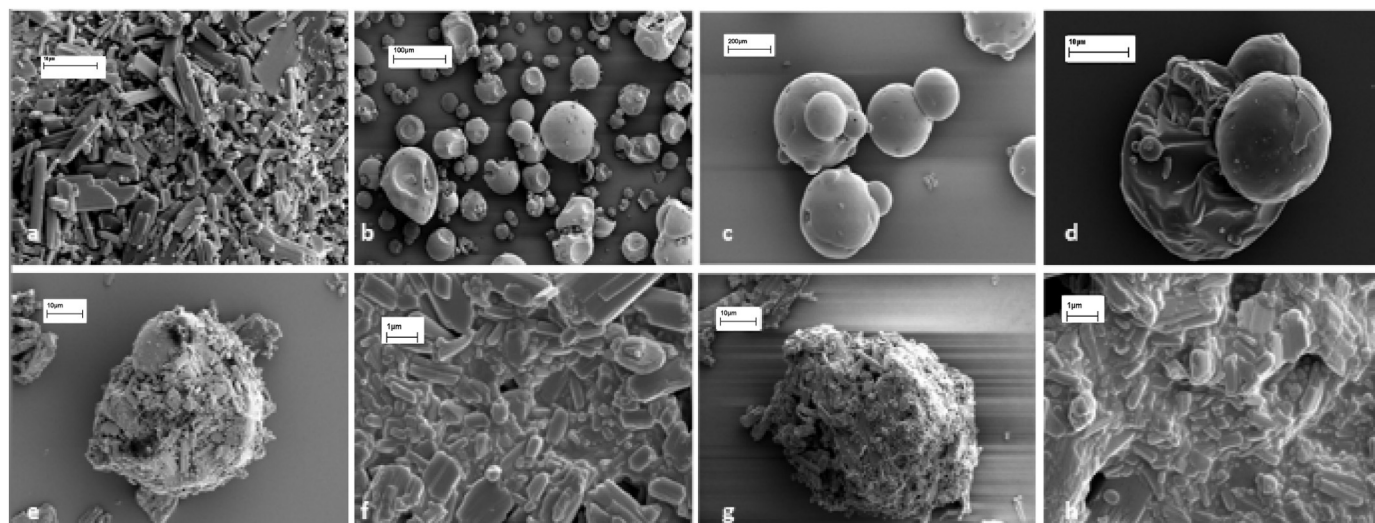


Fig. 3. SEM micrographs of raw PZQ (a), PVP (b), P188 (c), MDX (d), F4 PM (e), F4 dispersion (f), F3 PM (g) and F3 dispersion (h).

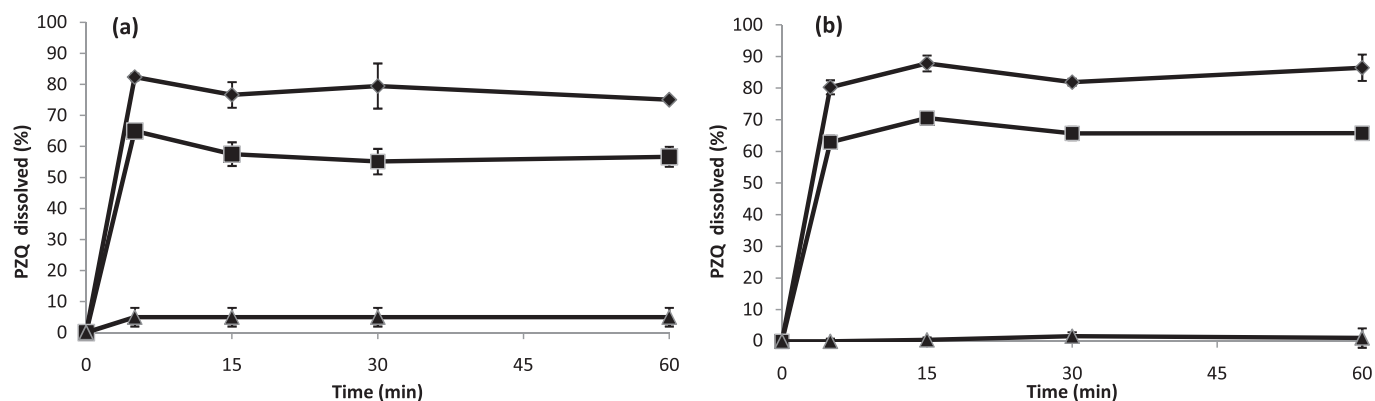


Fig. 4. Dissolution profiles
Dissolution profiles of raw PZQ (▲), F3 dispersion (■) and F4 dispersion (◆) in pH 7.4 buffer phosphate (a) and 0.1 N hydrochloric acid (b).

Table 3
Dissolution profile statistical comparison.

Dissolution medium	Dispersion	k (min ⁻¹) ^a	p-Value ^b	D.E. (%) ^a	p-Value ^b
pH 7.4 PB	F3	-0.026 ± 0.003	0.0262	55.02 ± 3.22	0.0076
	F4	-0.049 ± 0.011		72.51 ± 5.17	
0.1 N HCl	F3	-0.072 ± 0.004	0.0028	63.88 ± 7.60	0.0323
	F4	-0.128 ± 0.014		78.99 ± 2.87	

^a Results were expressed as mean value ± SD.

^b p-Value represents the statistical significance of the evaluation. Values lower than 0.05 indicate the existence of “significant differences” between samples, whereas values lower than 0.01 indicate “highly significant differences”.

4. Conclusion

Two formulations of PZQ, stabilized with P188 and PVP or MDX, were developed by HPH methodology. This technique had shown to be a robust and not complex process for particle size reduction, leading to a significant enhancement of PZQ dissolution rate. Furthermore, PZQ crystallinity was partially preserved during the HPH process, which is an important factor to be considered for formulation stability features. It is worth to mention that improved dissolution profiles were achieved, even maintaining some degree of PZQ crystallinity. In addition, oral bioavailability might be improved due to elongated-shaped particles, which will increase cellular uptake and transport across the intestinal membrane. Considering the overall results, it could be concluded that F4 is the formulation with best optimized parameters.

Future studies will be performed, in order to evaluate the applicability and versatility of the developed formulation to solid and liquid pharmaceutical products, with preserved properties, as well as alternative administration routes for specific types of parasitic diseases treatment.

Acknowledgments

The authors kindly thank Universidad Nacional del Sur (UNS, Argentina) (PGI 24/ZB70, PGI 24/B209) and Consejo Nacional de Investigaciones Científicas y Técnicas (CONICET, Argentina) (Res. 3646/14 and 11220150100704CO-D111/16) for the financial support; and Lic. Fernanda Cabrera (PLAPIQUI) and Pharm. Walter J. Starkloff (CONICET-UNS) for their technical assistance. Maria A. Gonzalez is grateful to CONICET for the PhD fellowship.

Conflicts of interest

The authors report no declarations of interest.

References

- [1] H.I. El-Subbagh, A.A. Al-Badr, Praziquantel, in: Florey (Ed.), *Analytical Profiles of Drug Substances and Excipients*, 24 Academic Press Inc., 1998, pp. 463–500.
- [2] R.D. Pearson, R.L. Guerrant, Praziquantel: a major advance in anthelmintic therapy, *Ann. Intern. Med.* 99 (2) (1983) 195–198, <https://doi.org/10.7326/0003-4819-99-2-195>.
- [3] CDC, Centers for disease control and prevention. Parasites—schistosomiasis, Treatment. (2012), <http://www.cdc.gov/parasites/schistosomiasis/treatment.html>, Accessed date: 14 May 2018.
- [4] WHO, World Health Organization. Schistosomiasis, Strategy (2016), <http://www.who.int/schistosomiasis/strategy/en/>, Accessed date: 14 May 2018.
- [5] K. Patzschke, J. Putter, L.A. Wegner, F.A. Horster, H.W. Diekmann, Serum concentrations and renal excretion in humans after oral administration of praziquantel - results of three determination methods, *Eur. J. Drug Metab. Pharmacokinet.* 4 (3) (1979) 149–156, <https://doi.org/10.1007/BF03189418>.
- [6] S.F. Sanchez Bruni, D.G. Jones, Q.A. Mckellar, Pharmacological approaches towards rationalizing the use of endoparasitic drugs in small animals, *J. Vet. Pharmacol. Ther.* 29 (6) (2006) 443–457, <https://doi.org/10.1111/j.1365-2885.2006.00806.x>.
- [7] M. Lindenberg, S. Kopp, J.B. Dressman, Classification of orally administered drugs on the World Health Organization model list of essential medicines according to the biopharmaceutics classification system, *Eur. J. Pharm. Biopharm.* 58 (2) (2004) 265–278, <https://doi.org/10.1016/j.ejpb.2004.03.001>.
- [8] L.Z. Benet, F. Broccatelli, T.I. Oprea, BDDCS applied to over 900 drugs, *AAPS J.* 13 (4) (2011) 519–547, <https://doi.org/10.1208/s12248-011-9290-9>.
- [9] W.J. Starkloff, V. Bucalá, S.D. Palma, N.L. Gonzalez Vidal, Design and in vitro characterization of ivermectin nanocrystals liquid formulation based on a top-down approach, *Pharm. Dev. Technol.* 22 (6) (2017) 809–817, <https://doi.org/10.1080/10837450.2016.1200078>.
- [10] R.H. Müller, C. Jacobs, O. Kayser, Nanosuspensions as particulate drug formulations in therapy rationale for development and what we can expect for the future, *Adv. Drug Deliv. Rev.* 47 (1) (2001) 3–19, [https://doi.org/10.1016/S0169-409X\(00\)00118-6](https://doi.org/10.1016/S0169-409X(00)00118-6).
- [11] A.A. Noyes, W.R. Whitney, The rate of solution of solid substances in their own solutions, *J. Am. Chem. Soc.* 19 (12) (1897) 930–934, <https://doi.org/10.1021/ja02086a003>.
- [12] L.D. Silva, E.C. Arrúa, D.A. Pereira, C.M. Fraga, T.L. Costa, A. Hemphill, C.J. Salomon, M.C. Vinaud, Elucidating the influence of praziquantel nanosuspensions on the in vivo metabolism of *Taenia crassiceps* cysticerci, *Acta Trop.* 161 (2016) 100–105, <https://doi.org/10.1016/j.actatropica.2016.06.002>.
- [13] R.H. Müller, K. Peters, Nanosuspensions for the formulation of poorly soluble drugs: I. Preparation by a size-reduction technique, *Int. J. Pharm.* 160 (2) (1998) 229–237, [https://doi.org/10.1016/S0378-5173\(97\)00311-6](https://doi.org/10.1016/S0378-5173(97)00311-6).
- [14] S. Verma, R. Gokhale, D.J. Burgess, A comparative study of top-down and bottom-up approaches for the preparation of micro/nanosuspensions, *Int. J. Pharm.* 380 (1–2) (2009) 216–222, <https://doi.org/10.1016/j.ijpharm.2009.07.005>.

- [15] S. Verma, S. Kumar, R. Gokhale, D.J. Burgess, Physical stability of nanosuspensions: investigation of the role of stabilizers on Ostwald ripening, *Int. J. Pharm.* 406 (1–2) (2011) 145–152, <https://doi.org/10.1016/j.ijpharm.2010.12.027>.
- [16] C.M. Keck, R.H. Müller, Drug nanocrystals of poorly soluble drugs produced by high-pressure homogenization, *Eur. J. Pharm. Biopharm.* 62 (1) (2006) 3–16, <https://doi.org/10.1016/j.ejpb.2005.05.009>.
- [17] E. Merisko-Liversidge, G.G. Liversidge, E.R. Cooper, Nanosizing: a formulation approach for poorly-water-soluble compounds, *Eur. J. Pharm. Sci.* 18 (2) (2003) 113–120, [https://doi.org/10.1016/S0928-0987\(02\)00251-8](https://doi.org/10.1016/S0928-0987(02)00251-8).
- [18] B.E. Rabinow, Nanosuspensions in drug delivery, *Nat. Rev. Drug Discov.* 3 (9) (2004) 785–796, <https://doi.org/10.1038/nrd1494>.
- [19] P. De la Torre, S. Torrado, S. Torrado, Preparation, dissolution and characterization of praziquantel solid dispersions, *Chem. Pharm. Bull.* 47 (11) (1999) 1629–1633, <https://doi.org/10.1248/cpb.47.1629>.
- [20] G. Becket, L.J. Schep, M.Y. Tan, Improvement of the in vitro dissolution of praziquantel by complexation with α -, β - and γ -cyclodextrins, *Int. J. Pharm.* 179 (1) (1999) 65–71, [https://doi.org/10.1016/S0378-5173\(98\)00382-2](https://doi.org/10.1016/S0378-5173(98)00382-2).
- [21] S.K. El-Arini, H. Leuenberger, Dissolution properties of praziquantel- β -cyclodextrin systems, *Pharm. Dev. Technol.* 1 (3) (1996) 307–315, <https://doi.org/10.3109/10837459609022600>.
- [22] S. Xie, B. Pan, B. Shi, Z. Zhang, X. Zhang, M. Wang, W. Zhou, Solid lipid nanoparticle suspension enhanced the therapeutic efficacy of praziquantel against tapeworm, *Int. J. Nanomedicine* 6 (2011) 2367–2374, <https://doi.org/10.2147/IJN.S24919>.
- [23] R.M. Mainardes, R.C. Evangelista, PLGA nanoparticles containing praziquantel: effect of formulation variables on size distribution, *Int. J. Pharm.* 290 (1–2) (2005) 137–144, <https://doi.org/10.1016/j.ijpharm.2004.11.027>.
- [24] L. Cheng, S. Guo, W. Wu, Characterization and in vitro release of praziquantel from poly (*e*-caprolactone) implants, *Int. J. Pharm.* 377 (1–2) (2009) 112–119, <https://doi.org/10.1016/j.ijpharm.2009.05.007>.
- [25] M. Čušovčan, J. Jablan, J. Lovrić, D. Cinić, N. Galić, M. Jug, Biopharmaceutical characterization of praziquantel cocrystals and cyclodextrin complexes prepared by grinding, *J. Pharm. Biomed. Anal.* 137 (2017) 42–53, <https://doi.org/10.1016/j.jpba.2017.01.025>.
- [26] N. El-Lakkany, S.H. Seif El-Din, L. Heikal, Bioavailability and in vivo efficacy of a praziquantel-polyvinylpyrrolidone solid dispersion in *Schistosoma mansoni*-infected mice, *Eur. J. Drug Metab. Pharmacokinet.* 37 (4) (2012) 289–299, <https://doi.org/10.1007/s13318-012-0089-6>.
- [27] N. Passerini, B. Albertini, B. Perissutti, L. Rodriguez, Evaluation of melt granulation and ultrasonic spray congealing as techniques to enhance the dissolution of praziquantel, *Int. J. Pharm.* 318 (1–2) (2006) 92–102, <https://doi.org/10.1016/j.ijpharm.2006.03.028>.
- [28] S.K. El-Arini, H. Leuenberger, Dissolution properties of praziquantel-PVP systems, *Pharm. Acta Helv.* 73 (2) (1998) 89–94, [https://doi.org/10.1016/S0031-6865\(97\)00051-4](https://doi.org/10.1016/S0031-6865(97)00051-4).
- [29] *British Pharmacopoeia, The Stationary Office Medicinal and Pharmaceutical Substances, Vol. I & II* (2009) London.
- [30] U.S. Department of Health and Human Services, U.S. Food & Drug Administration. Inactive ingredient database, Available in <https://www.accessdata.fda.gov/scripts/cder/iig/index.cfm>, Accessed date: 14 May 2018.
- [31] V.G. Kadajji, G.V. Betageri, Water soluble polymers for pharmaceutical applications, *Polymer* 3 (2011) 1972–2009, <https://doi.org/10.3390/polym3041972>.
- [32] E.D. Costa, J. Priotti, S. Orlandi, D. Leonardi, M.C. Lamas, T.G. Nunes, H.P. Diogo, C.J. Salomon, M.J. Ferreira, Unexpected solvent impact in the crystallinity of praziquantel/poly (vinylpyrrolidone) formulations. A solubility, DSC and solid-state NMR study, *Int. J. Pharm.* 511 (2) (2016) 983–993, <https://doi.org/10.1016/j.ijpharm.2016.08.009>.
- [33] Y. Wang, Y. Zheng, L. Zhang, Q. Wang, D. Zhang, Stability of nanosuspensions in drug delivery, *J. Control. Release* 172 (3) (2013) 1126–1141, <https://doi.org/10.1016/j.jconrel.2013.08.006>.
- [34] *Malvern, Malvern Instruments (Ed.), Zetasizer Nano Series User Manual, 2004.*
- [35] *The United States Pharmacopoeia and National Formulary, USP 30-NF 25, Spanish Edition, The United States Pharmacopoeial Convention, Inc., Rockville, MD, 2007, pp. 1362–1363.*
- [36] K.A. Khan, The concept of dissolution efficiency, *J. Pharm. Pharmacol.* 27 (1) (1975) 48–49, <https://doi.org/10.1111/j.2042-7158.1975.tb09378.x>.
- [37] Y. Liu, X. Wang, J.K. Wang, C.B. Ching, Structural characterization and Enantioseparation of the chiral compound praziquantel, *J. Pharm. Sci.* 93 (12) (2004) 3039–3046, <https://doi.org/10.1002/jps.20211>.
- [38] D.T. Turner, A. Schwartz, The glass transition temperature of poly (N-vinyl pyrrolidone) by differential scanning calorimetry, *Polymer* 26 (5) (1985) 757–762, [https://doi.org/10.1016/0032-3861\(85\)90114-4](https://doi.org/10.1016/0032-3861(85)90114-4).
- [39] M. Nawa, K.H. Bhandari, D.X. Li, T.H. Kwon, J.A. Kim, B.K. Yoo, J.S. Woo, W.S. Lyoo, C.S. Yong, H.G. Choi, Preparation, characterization and in vivo evaluation of ibuprofen binary solid dispersions with poloxamer 188, *Int. J. Pharm.* 343 (1–2) (2007) 228–237, <https://doi.org/10.1016/j.ijpharm.2007.05.031>.
- [40] M.J. Mollan Jr., M. Celik, Maltodextrin, in: Florey (Ed.), *Analytical Profiles of Drug Substances and Excipients*, 24 Academic Press Inc., 1996, pp. 307–349.
- [41] P. Mura, M.T. Faucci, A. Manderioli, G. Bramanti, L. Ceccarelli, Compatibility study between ibuprofen and pharmaceutical excipients using differential scanning calorimetry, hot-stage microscopy and scanning electron microscopy, *J. Pharm. Biomed. Anal.* 18 (1–2) (1998) 151–163, [https://doi.org/10.1016/S0731-7085\(98\)00171-X](https://doi.org/10.1016/S0731-7085(98)00171-X).
- [42] B. Tița, A. Fuliș, G. Bandur, E. Marian, D. Tița, Compatibility study between ketoprofen and pharmaceutical excipients used in solid dosage forms, *J. Pharm. Biomed. Anal.* 56 (2) (2011) 221–227, <https://doi.org/10.1016/j.jpba.2011.05.017>.
- [43] D. Hasa, D. Voinovich, B. Perissutti, G. Grassi, S. Fiorentino, R. Farra, M. Abrami, I. Colombo, M. Grassi, Reduction of melting temperature and enthalpy of drug crystals: theoretical aspects, *Eur. J. Pharm. Sci.* 50 (1) (2013) 17–28, <https://doi.org/10.1016/j.ejps.2013.03.018>.
- [44] C. Kuehl, N. El-Gendy, C. Berkland, NanoClusters surface area allows nanoparticle dissolution with microparticle properties, *J. Pharm. Sci.* 103 (6) (2014) 1787–1798, <https://doi.org/10.1002/jps.23980>.
- [45] M. Yoshioka, B. Hancock, G. Zografi, Inhibition of Indomethacin crystallization in poly(vinylpyrrolidone) coprecipitates, *J. Pharm. Sci.* 84 (8) (1995) 983–986, <https://doi.org/10.1002/jps.2600840814>.
- [46] L. Taylor, G. Zografi, Spectroscopic characterization of interactions between and indomethacin in amorphous molecular dispersions, *Pharm. Res.* 14 (12) (1997) 1691–1698, <https://doi.org/10.1023/A:1012167410376>.
- [47] V. Tantishaiyakul, N. Kaewnopparat, S. Ingkawatwornwong, Properties of solid dispersions of piroxicam in polyvinylpyrrolidone K-30, *Int. J. Pharm.* 143 (1) (1996) 59–66, [https://doi.org/10.1016/S0378-5173\(96\)04687-X](https://doi.org/10.1016/S0378-5173(96)04687-X).
- [48] P. Sharma, W. Denny, S. Garg, Effect of wet milling process on the solid state of indomethacin and simvastatin, *Int. J. Pharm.* 380 (1–2) (2009) 40–48, <https://doi.org/10.1016/j.ijpharm.2009.06.029>.
- [49] B. Perissutti, N. Passerini, R. Trastullo, J. Keiser, D. Zanolla, G. Zingone, D. Voinovich, B. Albertini, An explorative analysis of process and formulation variables affecting commilling in a vibrational mill: the case of praziquantel, *Int. J. Pharm.* 533 (2) (2017) 402–412, <https://doi.org/10.1016/j.ijpharm.2017.05.053>.
- [50] V. Bühler, Polyvinylpyrrolidone – Excipients for Pharmaceuticals, Springer, Germany, 2005, p. 87, <https://doi.org/10.1007/b138598>.
- [51] L. Yu, Amorphous pharmaceutical solids: preparation, characterization and stabilization, *Adv. Drug Deliv. Rev.* 48 (1) (2001) 27–42, [https://doi.org/10.1016/S0169-409X\(01\)00098-9](https://doi.org/10.1016/S0169-409X(01)00098-9).
- [52] D.A. Alshora, M.A. Ibrahim, F.K. Alanazi, Nanotechnology from particle size reduction to enhancing aqueous solubility, in: A.M. Grumezescu (Ed.), *Surface Chemistry of Nanobiomaterials*, Elsevier, 2016, pp. 163–191, <https://doi.org/10.1016/B978-0-323-42861-3.00006-6> Chapter 6.
- [53] I. Ghosh, S. Bose, R. Vipagunta, F. Harmon, Nanosuspension for improving the bioavailability of a poorly soluble drug and screening of stabilizing agents to inhibit crystal growth, *Int. J. Pharm.* 409 (1–2) (2011) 260–268, <https://doi.org/10.1016/j.ijpharm.2011.02.051>.
- [54] R.C. Rowe, P.J. Sheskey, S.C. Owen (Eds.), *Handbook of Pharmaceutical Excipients, 5th Ed.*, 430–433 Pharmaceutical Press, London, 2006.
- [55] A. Banerjee, J. Qi, R. Gongoi, J. Wong, S. Mitragotri, Role of nanoparticle size, shape and surface chemistry in oral drug delivery, *J. Control. Release* 238 (2016) 176–185, <https://doi.org/10.1016/j.jconrel.2016.07.051>.
- [56] P. Kocbek, S. Baumgartner, J. Kristl, Preparation and evaluation of nanosuspensions for enhancing the dissolution of poorly soluble drugs, *Int. J. Pharm.* 312 (1–2) (2006) 179–186, <https://doi.org/10.1016/j.ijpharm.2006.01.008>.
- [57] F. Lai, E. Pini, G. Angioni, M.L. Manca, J. Perricci, C. Sinico, A.M. Fadda, Nanocrystals as tool to improve piroxicam dissolution rate in novel orally disintegrating tablets, *Eur. J. Pharm. Biopharm.* 79 (3) (2011) 552–558, <https://doi.org/10.1016/j.ejpb.2011.07.005>.
- [58] R. Mauludin, R.H. Müller, C.M. Keck, Kinetic solubility and dissolution velocity of rutin nanocrystals, *Eur. J. Pharm. Sci.* 36 (4–5) (2009) 502–510, <https://doi.org/10.1016/j.ejps.2008.12.002>.
- [59] M. Guo, Q. Fu, C. Wu, Z. Guo, M. Li, J. Sun, Z. He, L. Yang, Rod shaped nanocrystals exhibit superior in vitro dissolution and in vivo bioavailability over spherical like nanocrystals: a case study of lovastatin, *Colloids Surf. B: Biointerfaces* 128 (2015) 410–418, <https://doi.org/10.1016/j.colsurfb.2015.02.039>.
- [60] S.L. Lee, A.S. Raw, L. Yu, Dissolution testing, in: R. Krishna, L. Yu (Eds.), *Biopharmaceutical Applications in Drug Development*, Springer, Boston, MA, 2008, pp. 47–74, <https://doi.org/10.1007/978-0-387-72379-2>.



María Alejandra González is a pharmacist graduated from Universidad Nacional del Sur (Argentina) and a doctoral fellowship holder of Consejo Nacional de Investigaciones Científicas y Técnicas (CONICET, Argentina). Teacher assistant in Pharmaceutical Technology cathedra at Universidad Nacional del Sur (Argentina). Research Interests: Pharmaceutical materials and processing.



María Verónica Ramírez Rigo is a professor of the Department of Biology, Biochemistry, Pharmacy at Universidad Nacional del Sur and a Scientific Researcher of CONICET (Consejo Nacional de Investigaciones Científicas y Técnicas, Argentina). Dipl.-Pharmaceutics and PhD. in Chemical Science, Universidad Nacional de Córdoba (Córdoba, Argentina). Research Interests: Pharmaceutical materials and processing, Powder Technology, Drug delivery.



Noelia Gonzalez Vidal. Pharmacist and PhD. of Buenos Aires University, in Pharmaceutical Technology area. *Teaching*: Full Professor, in charge of Quality Control of Pharmaceutical cathedra and two courses for PhD. programs. *Research*: Assistant Researcher, CONICET. Director of research projects and researcher in a technology transfer project. *University Management*: Titular member of Academic Committee of Postgraduate Programs in Pharmacy. Titular member of Departmental Council. Vice-Dean (2013–2015, and April 2016–March 2017).